Chiral and deconfinement thermal transitions at finite quark spin density in lattice QCD

Artem Roenko[1],

in collaboration with

V. Braguta, M. Chernodub,

[1] Joint Institute for Nuclear Research, Bogoliubov Laboratory of Theoretical Physics
roenko@theor.jinr.ru

International Workshop "Infinite and Finite Nuclear Matter" (INFINUM-2025),
Dubna, JINR, 12 – 16 May 2025

based on arXiv:2503.18636 [hep-lat]

- In non-central heavy ion collisions the droplets of QGP with angular momentum are created.
- An interplay between rotation, vorticity, and spins of quarks lead to series of effects in HIC.
- The rotation occurs with relativistic velocities. $\Rightarrow$ Spin alignment of created particles.

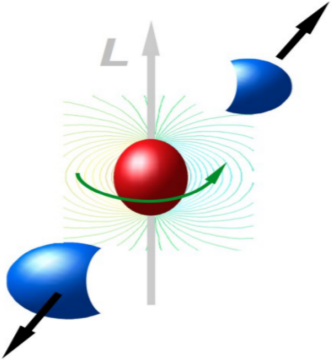

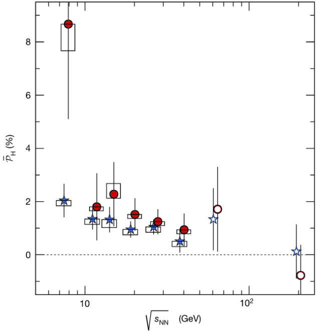

[L. Adamczyk et al. (STAR), Nature **548**, 62–65 (2017), arXiv:1701.06657 [nucl-ex]]

$\langle\omega\rangle \sim 7$ MeV $\quad (\sqrt{s_{NN}}$-averaged)

Spin potential

We introduce the finite spin density of quarks by analogy with the finite quark density

- Quark chemical potential, μ_q $\longleftrightarrow$ quark number density, $\bar{\psi}\gamma^0\psi$,

  An additional term in the Dirac Lagrangian:

$$\delta_N \mathcal{L}_q = \mu_q \, \bar{\psi}\gamma^0\psi \, , \tag{1}$$

- Spin potential, μ_Σ $\longleftrightarrow$ density of quark spin, $\bar{\psi}\gamma^0\Sigma^{12}\psi$,

  An additional term in the Dirac Lagrangian:

$$\delta_\Sigma \mathcal{L}_q = \mu_\Sigma \, \bar{\psi}\gamma^0\Sigma^{12}\psi \, . \tag{2}$$

- In general form (we use canonical definition of spin tensor),

$$\delta_\Sigma \, \mathcal{L}_q = \mu_{\alpha,\mu\nu} \, \overline{\psi}\mathcal{S}^{\alpha,\mu\nu}\psi \, , \qquad \text{where} \quad \mathcal{S}^{\alpha,\mu\nu} = \frac{1}{2}\left\{\gamma^\alpha, \Sigma^{\mu\nu}\right\}, \qquad \Sigma^{\mu\nu} = \frac{i}{4}\left[\gamma^\mu, \gamma^\nu\right], \tag{3}$$

  but we consider the spins of quarks polarized along the z axis, $\mu_{\alpha,\mu\nu} = \dfrac{\mu_\Sigma}{2}\delta_{\alpha 0}\left(\delta_{\mu 1}\delta_{\nu 2} - \delta_{\nu 1}\delta_{\mu 2}\right)$.

- Spin potential expresses a tendency to favor one spin state over the other, $\mu_\Sigma = \delta E_\uparrow - \delta E_\downarrow$.

QCD on the lattice

Our aim is to study QCD phase diagram for finite spin density, μ_Σ, on the lattice.

Lattice simulation is a powerful method to study strong-interacting systems:

- Based on the *path-integral* representation of the partition function (Euclidean action is used):

$$\mathcal{Z} = \int \mathcal{D}[U]\mathcal{D}[\psi,\bar{\psi}]\; e^{-S_G(U)-S_F(\psi,\bar{\psi},U)} = \int \mathcal{D}[U]\; e^{-S_G(U)} \prod_f \det[M^{(f)}(\psi,\bar{\psi},U)]\,,$$

$$\langle \mathcal{O} \rangle = \frac{1}{\mathcal{Z}} \int \mathcal{D}[U]\,\mathcal{O}(\psi,\bar{\psi},U)\; e^{-S_G(U)} \prod_f \det[M^{(f)}(\psi,\bar{\psi},U)] \approx \frac{1}{N_{\text{conf}}} \sum_{\substack{i=1 \\ P[U_i]\,\propto\, e^{-S}}}^{N_{\text{conf}}} O[\text{conf}_i]\,.$$

- The spacetime is discretized on the hypercubic Euclidean lattice with finite spacing a.
- The integrals are computed using Monte-Carlo algorithms. HPC is needed.
- The results should be finite in the continuum limit $a \to 0$.
- Statistical and systematic uncertainties are under control.

Our aim is to study QCD phase diagram for finite spin density, μ_Σ, on the lattice.

Lattice simulation is a powerful method to study strong-interacting systems:

- Based on the *path-integral* representation of the partition function (Euclidean action is used):

$$\mathcal{Z} = \int \mathcal{D}[U]\mathcal{D}[\psi,\bar{\psi}]\ e^{-S_G(U)-S_F(\psi,\bar{\psi},U)} = \int \mathcal{D}[U]\ e^{-S_G(U)} \prod_f \det[M^{(f)}(\psi,\bar{\psi},U)]\,,$$

$$\langle \mathcal{O} \rangle = \frac{1}{\mathcal{Z}} \int \mathcal{D}[U]\,\mathcal{O}(\psi,\bar{\psi},U)\ e^{-S_G(U)} \prod_f \det[M^{(f)}(\psi,\bar{\psi},U)] \approx \frac{1}{N_{\text{conf}}} \sum_{\substack{i=1 \\ P[U_i]\propto e^{-S}}}^{N_{\text{conf}}} O[\text{conf}_i]\,.$$

- The spacetime is discretized on the hypercubic Euclidean lattice with finite spacing a.
- The integrals are computed using Monte-Carlo algorithms. HPC is needed.
- The results should be finite in the continuum limit $a \to 0$.
- Statistical and systematic uncertainties are under control.

The sign problem arises for finite μ_Σ, like for finite μ_B.

In the imaginary time formalism, the quark spin potential becomes an imaginary quantity after the Wick rotation, similarly to the baryon chemical potential,

$$\mu_\Sigma = i\mu_\Sigma^{\mathrm{I}} \,. \tag{4}$$

We aim to find the curvature κ_Σ of the deconfinement ($\ell = L$) and chiral ($\ell = \psi$) phase transitions:

$$\frac{T_c^\ell(\mu_\Sigma^{\mathrm{I}})}{T_c^\ell(0)} = 1 + \kappa_\Sigma^\ell \left(\frac{\mu_\Sigma^{\mathrm{I}}}{T_c(0)} \right)^2 + \dots\,, \qquad [\ell = L, \psi]\,, \tag{5}$$

and after analytic continuation we get,

$$\frac{T_c^\ell(\mu_\Sigma)}{T_c(0)} = 1 - \kappa_\Sigma^\ell \left(\frac{\mu_\Sigma}{T_c(0)} \right)^2 + \dots\,, \qquad [\ell = L, \psi]\,. \tag{6}$$

The spin curvature κ_Σ describes how the presence of small quark density affects the transitions in QCD.

Quark chemical potential

There are analogies with other “potentials” in QCD:

Quark chemical potential, μ_q

$$\delta_N \mathcal{L}_q = \mu_q \bar{\psi}\gamma^0\psi \equiv \mu_q j^0 .$$

Usually the chemical potentials with respect to the conserved charges $B, S, Q, \ldots$ are used instead:

- Baryon chemical potential

  $\mu_u = \mu_d \simeq \mu_B/3 = \mu_l, \quad \mu_s = 0$

  (simulation with imaginary $\mu_{l,I}$)

  T_c decreases with real μ_B.
  $\kappa_q = 9\kappa_B = 0.12(2)$.

  [C. Bonati et al., Phys. Rev. D **92**, 054503 (2015), arXiv:1507.03571 [hep-lat]]

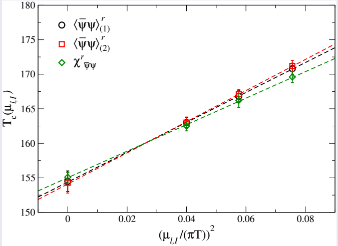

- Isospin chemical potential

  $\mu_u = \mu_I, \quad \mu_d = -\mu_I$ (no sign problem) $\Rightarrow$ T_c decreases with μ_I.

  [B. B. Brandt, G. Endrodi, and S. Schmalzbauer, Phys. Rev. D **97**, 054514 (2018), arXiv:1712.08190 [hep-lat]]

Chiral chemical potential vs spin potential

Chiral (axial) chemical potential, μ_5

$$\delta_A \mathcal{L}_q = \mu_5\, \bar{\psi}\gamma^0\gamma^5\psi \equiv \mu_5\, j_A^0 \,.$$

(no sign problem)

T_c increases with real μ_5.

[V. V. Braguta et al., Phys. Rev. D **93**, 034509 (2016), arXiv:1512.05873 [hep-lat]]

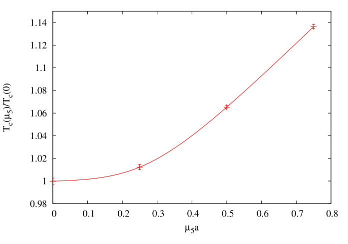

Spin potential, μ_Σ

$$\delta_\Sigma \mathcal{L}_q = \mu_\Sigma\, \bar{\psi}\gamma^0\Sigma^{12}\psi = \frac{1}{2}\mu_\Sigma\, \bar{\psi}\gamma^3\gamma^5\psi \;\leftrightarrow\; \frac{1}{2}\mu_\Sigma\, j_A^3 \,.$$

(simulation with imaginary μ_Σ^{I})

At $T = 0$, the effects of $\mu_\Sigma^{\mathrm{I}} \;\leftrightarrow\; \mu_5 = \mu_\Sigma/2 \quad \Rightarrow$ we expect that T_c increases with μ_Σ^{I},
or, T_c decreases with real μ_Σ

Rigid rotation vs spin potential

The spin potential μ_Σ is somewhat similar to the angular velocity Ω of a uniformly rotating system:

Angular velocity, Ω

$$\delta_\Omega \mathcal{L}_q = \Omega\,\bar{\psi}\big[i(-x\partial_y + y\partial_x) + \gamma^0\Sigma^{12}\big]\psi\,,$$

$$\delta_\Omega \mathcal{L}_G = \frac{1}{2g^2}\Big[2r\Omega\left(F^a_{\hat{\varphi}r}F^a_{rt} + F^a_{\hat{\varphi}z}F^a_{zt}\right) - r^2\Omega^2\left(F^a_{\hat{\varphi}z}F^a_{\hat{\varphi}z} + F^a_{r\hat{\varphi}}F^a_{r\hat{\varphi}}\right)\Big],$$

(simulation with imaginary Ω_I)

▷ At the rotation axis, $x = y = 0$, the local action of rotating system coincides with the system at finite spin density of quarks, $\Omega = \mu_\Sigma$.

▷ The results for finite μ_Σ describes the shift of T_c at $r = 0$ for mixed phase in rotating QCD, if we expect the validity of "local thermalization".

▷ The system at finite μ_Σ is homogeneous, unlike the case of rigid rotation.

Lattice action and setup

In continuum notations, the Euclidean quark action at the finite spin potential μ_Σ has the following form:

$$S_F = \int d^4x \, \bar{\psi}\Big[\gamma^x D_x + \gamma^y D_y + \gamma^z D_z + \gamma^\tau \big(D_\tau + i\mu_\Sigma^{\mathrm{I}} \Sigma^{12}\big) + m\Big]\psi \,. \tag{7}$$

- We use $N_f = 2$ clover-improved Wilson fermions (c_{SW} from one-loop) + RG-improved (Iwasaki) gauge action.
- The spin density term is exponentiated like chemical potential.
- Simulations are performed on lattices of the size 4×16^3, 5×20^3, 6×24^3 for meson mass ratios $m_{\mathrm{PS}}/m_{\mathrm{V}} = 0.60, \ldots, 0.85$.
- Due to competition between quarks and gluons in rotating system, the dependence of the results on the pion mass is of a particular interest.
- Temperature is $T = 1/(N_t a)$.

Deconfinement crossover

In QCD, the Polyakov loop is an approximate order parameter,

$$L = \frac{1}{N_s^3} \sum_{\vec{r}} \mathrm{Tr} \left[\prod_{\tau=0}^{N_t-1} U_4(\vec{r}, \tau) \right], \tag{8}$$

In confinement $\langle L \rangle \approx 0$; in deconfinement $\langle L \rangle \neq 0$. $\langle L \rangle = e^{-F_Q/T}$

The deconfinement critical temperature is associated with the peak of the Polyakov loop susceptibility

$$\chi_L = \langle |L|^2 \rangle - \langle |L| \rangle^2 . \tag{9}$$

Chiral crossover

The chiral critical temperature is determined using the (disconnected) chiral susceptibility:

$$\chi_{\bar{\psi}\psi}^{\mathrm{disc}} = \frac{N_f T}{V} \left[\left\langle \mathrm{Tr}(M^{-1})^2 \right\rangle - \left\langle \mathrm{Tr}(M^{-1}) \right\rangle^2 \right]. \tag{10}$$

At low temperatures chiral symmetry is broken, $\langle \bar{\psi}\psi \rangle \neq 0$, and it is restored at high temperatures $\langle \bar{\psi}\psi \rangle = 0$.

Polyakov loop

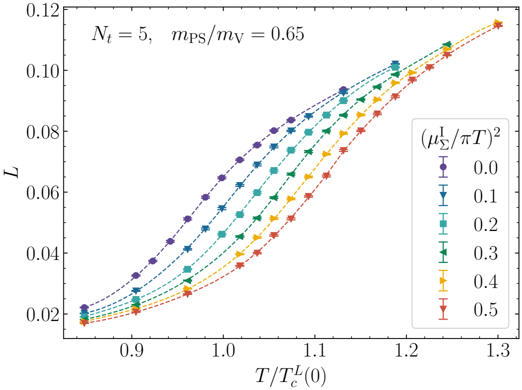

Figure: The Polyakov loop as a function of temperature T for various values of the (imaginary) spin potential μ_Σ^{I}.

- An increasing imaginary spin potential leads to a decrease of the Polyakov loop at fixed temperature.

Polyakov loop susceptibility and chiral susceptibility

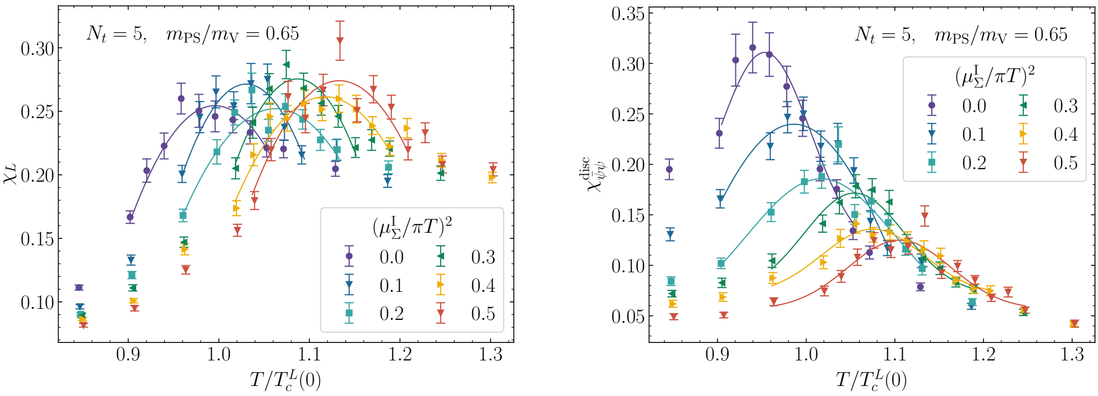

Figure: The susceptibilities of the Polyakov loop and the chiral condensate as a function of temperature.

- Pseudo-critical temperatures increases with an imaginary spin potential.
- The finite (imaginary) spin density softens the chiral phase transition.

Pseudo-critical temperatures: lattice spacing effects

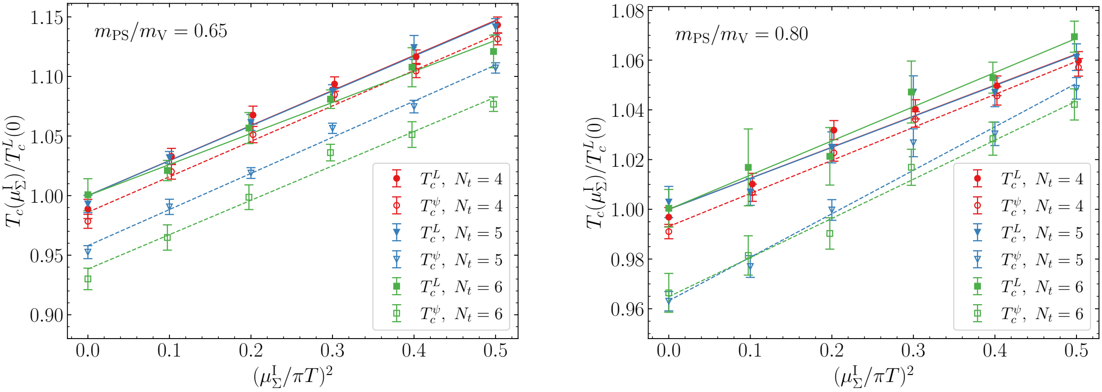

Figure: Transition temperatures T_c of the deconfinement and chiral crossovers as a function of spin potential.

- Pseudo-critical temperatures increases with an imaginary spin potential.
- There is a weak dependence of the results on the lattice spacing a.

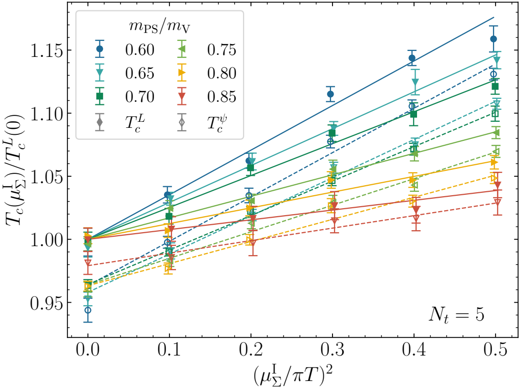

We fit the data by the quadratic function of the imaginary spin potential μ_Σ^{I}:

$$T_c^\ell(\mu_\Sigma^{\mathrm{I}}) = T_c^\ell(0)\left[1 + \kappa_\Sigma^\ell\left(\frac{\mu_\Sigma^{\mathrm{I}}}{T}\right)^2\right]. \qquad (11)$$

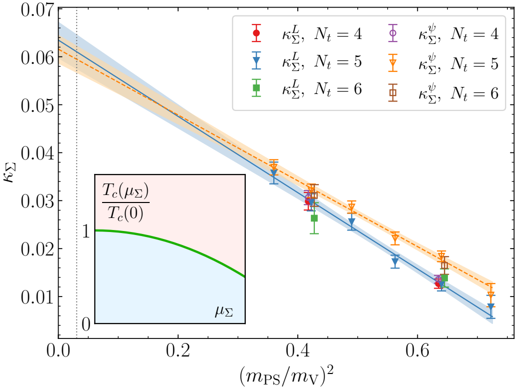

We fit the data by the quadratic function of the imaginary spin potential $\mu_\Sigma^{\rm I}$:

$$T_c^\ell(\mu_\Sigma^{\rm I}) = T_c^\ell(0)\left[1 + \kappa_\Sigma^\ell\left(\frac{\mu_\Sigma^{\rm I}}{T}\right)^2\right]. \qquad (11)$$

The dependence of the curvatures κ_Σ^ℓ ($\ell = L, \psi$) on the pion mass ratio can be well described by

$$\kappa_\Sigma^\ell(\xi) = k_\Sigma^\ell + \gamma_\Sigma^\ell\,\xi^2\,, \qquad \xi = \frac{m_{\rm PS}}{m_{\rm V}}\,. \qquad (12)$$

In the limit of physical pion mass,

$$\kappa_\Sigma^{L\ (\rm phys)} = 0.0610(35)\,, \qquad \kappa_\Sigma^{\psi\ (\rm phys)} = 0.0595(27)\,, \qquad \text{at} \quad \left(\frac{m_{\rm PS}}{m_{\rm V}}\right)_{\rm phys} = 0.175\ .$$

Conclusions

- We performed first-principle numerical simulations in the lattice QCD with $N_f = 2$ dynamical quarks to determine the effect of a finite spin density of quarks on the deconfinement and chiral transitions.
- The quark spin density leads to a decrease of the temperatures of the chiral and deconfinement crossover. The result is qualitatively similar to finite baryon density.
- The curvatures, κ_Σ^L and κ_Σ^ψ, sufficiently depend on the pion mass. At physical pion mass point they are approximately the same within a small statistical error, $\kappa_\Sigma^L \simeq \kappa_\Sigma^\psi \simeq 0.06$. For baryon potential, curvature is of the same order, $\kappa_q = 0.12(2)$.
- The presence of the background spin potential does not lead to a splitting of the deconfinement and chiral transitions.
- The small magnitude of the curvatures implies that for the phenomenologically relevant values of the spin potential $\mu_\Sigma = 10\,\text{MeV}$, the deconfinement and chiral transition temperatures drop only by about 0.03%.
- It allows us to estimate the rotational effects for the on-axis critical temperature in rotating QCD within approximation of local thermalization.

Thank you for your attention!

Lattice quark action

The $N_f = 2$ clover-improved action for Wilson fermions is

$$S_F = \sum_{f=u,d} \sum_{x_1,x_2} \bar{\psi}^f(x_1) M_{x_1,x_2} \psi^f(x_2)\,, \tag{13}$$

with the matrix

$$\begin{aligned} M_{x_1,x_2} = \delta_{x_1,x_2} - \kappa \Bigg[\sum_{\mu=x,y,z} \Big((1-\gamma^\mu) T_{\mu+} + (1+\gamma^\mu) T_{\mu-} \Big) + \\ + (1-\gamma^\tau) \exp\Big(ia\mu_\Sigma^{\mathrm{I}} \Sigma^{12} \Big) T_{\tau+} + +(1+\gamma^\tau) \exp\Big(-ia\mu_\Sigma^{\mathrm{I}} \Sigma^{12} \Big) T_{\tau-} \Bigg] - \delta_{x_1,x_2} c_{SW} \kappa \sum_{\mu<\nu} \sigma_{\mu\nu} F_{\mu\nu}\,, \end{aligned} \tag{14}$$

where $\kappa = 1/(8+2am)$, $T_{\mu+} = U_\mu(x_1)\delta_{x_1+\mu,x_2}$, $T_{\mu-} = U_\mu^\dagger(x_1)\delta_{x_1-\mu,x_2}$ and $F_{\mu\nu} = (\bar{U}_{\mu\nu} - \bar{U}_{\mu\nu}^\dagger)/8i$. For the clover coefficient, we adopt the mean-field value $c_{SW} = (1 - W^{1\times 1})^{-3/4} = (1 - 0.8412/\beta)^{-3/4}$.

We discretize the gluon part of the action using the renormalization-group improved (Iwasaki) lattice action, which is unaffected by spin density:

$$S_G = \beta \sum_x \left(c_0 \sum_{\mu<\nu} W_{\mu\nu}^{1\times1} + c_1 \sum_{\mu\neq\nu} W_{\mu\nu}^{1\times2} \right), \tag{15}$$

with the lattice couplings $\beta = 6/g^2$, $c_0 = 1 - 8c_1$, and $c_1 = -0.331$. The gauge field enters via

$$W_{\mu\nu}^{1\times1}(x) = 1 - \frac{1}{3} \mathrm{Re}\,\mathrm{Tr}\, \overline{U}_{\mu\nu}(x)\,, \tag{16}$$

$$W_{\mu\nu}^{1\times2}(x) = 1 - \frac{1}{3} \mathrm{Re}\,\mathrm{Tr}\, R_{\mu\nu}(x)\,, \tag{17}$$

where $\overline{U}_{\mu\nu}(x)$ denotes the clover-type average of four plaquettes and $R_{\mu\nu}(x)$ represents a rectangular loop.